Journal of Inorganic Biochemistry 240 (2023) 112092

Contents lists available at ScienceDirect

Journal of Inorganic Biochemistry

journal homepage: www.elsevier.com/locate/jinorgbio

Rhenium(I)-tricarbonyl complexes with methimazole and its selenium analogue: Syntheses, characterization and cell toxicity

Farideh Jalilehvand [a,*], Valerie Brunskill [a], Tran Si Bui Trung [a], Isbel Lopetegui-Gonzalez [b], Carrie S. Shemanko [b], Benjamin S. Gelfand [a], Jian-Bin Lin [a]

[a] Department of Chemistry, University of Calgary, Calgary, Alberta T2N 1N4, Canada
[b] Department of Biological Sciences, University of Calgary, Calgary, Alberta T2N 1N4, Canada

ARTICLE INFO

Keywords:
Rhenium(I) tricarbonyl diimine complexes
Methimazole
1-methylimidazole-2-selone
Structure
Spectroscopy
Cytotoxicity

ABSTRACT

This study explores the effect of a thione/selone ligand on the cell toxicity (*in vitro*) and light activity of diimine $Re(CO)_3^+$ complexes. Six rhenium(I) complexes with general formula *fac*-$[Re(CO)_3(N,N')X]^+$ were prepared, where X = 2-mercapto-1-methylimidazole (methimazole; MMI), and 1-methylimidazole-2-selone (MSeI); *N,N′* = 2,2′-bipyridine (bpy), 1,10-phenanthroline (phen) and 2,9-dimethyl-1,10-phenanthroline (dmphen). Their triflate salts were characterized using single-crystal X-ray diffraction, ^1H, ^{13}C and 2D NMR, UV–vis and vibrational spectroscopy. Their cytotoxic properties were tested, showing significant cytotoxicity (IC_{50} = 8.0–55 μM) towards the human breast cancer cell line MDA-MB-231. The half-inhibitory concentration (IC_{50}) for *fac*-$[Re(CO)_3(dmphen)(MMI)]^+$, the most toxic complex in this series (8.0 ± 0.2 μM), was comparable to that of the corresponding aqua complex *fac*-$[Re(CO)_3(dmphen)(H_2O)]^+$ with IC_{50} = 6.0 ± 0.1 μM. The *fac*-$[Re(CO)_3(bpy)(MMI/MSeI)]^+$ complexes were somewhat less toxic towards the human embryonic kidney cell line HEK-293 T after 48 h of exposure. The stability of the complexes upon irradiation was monitored using UV–vis spectroscopy, with no CO released when exposed to UV-A light (λ = 365 nm).

1. Introduction

Rhenium(I) diimine tricarbonyl complexes, *fac*-$[Re(CO)_3(N,N)X]^{+/0/-}$ where (*N,N*) = diimine and X = halide or an O, N, P or S-donor ancillary ligand, have attracted great attention in recent years for their versatile applications as catalysts [1,2], bio-imaging probes and potential drugs for cancer treatment [3–7]. Such Re(I) complexes are generally inert with slow ligand exchange rate due to the d^6 low-spin electron configuration, and are stable in a cellular environment [8,9]. Their properties can be finely tuned by changing the nature of the diimine and ancillary ligands [10], affecting their level of cytotoxicity and ability to target different cellular organelles [11–13]. Monitoring emissions from their long-lived ^{3}MLCT excited states (triplet state metal-to-ligand charge transfer) allows probing their cellular localization using confocal spectroscopy. The quantum yield of such emissions can be tuned by selecting the diimine and ancillary ligands [3]. The unique photophysical properties of some *fac*-$[Re(CO)_3(N,N)X]^{+/0}$ complexes make them excellent candidates as photodynamic therapy agents. These complexes are non-toxic in the dark at prescribed dosages, but when irradiated with visible light (penetrating deeper into tissue than UV), they emit luminescence that in presence of oxygen can generate reactive oxygen species (such as $^1O_2$) that can lead to cell death [14]. Others may exhibit photo-cytotoxic properties by releasing toxic CO molecules upon irradiation [15], especially *fac*-$[Re(CO)_3(N,N)(PR_3)]^+$ complexes where the ancillary phosphine group has a strong *trans*-directing influence [16,17].

Thus far, structures and properties of a few *fac*-$[Re(CO)_3(N,N)X]^{+/0/-}$ complexes with axial S-donor ligands have been investigated [18–29], but not for a Se-donor ligand. Previous results from our group have shown how replacement of an aqua ligand with a negatively charged cysteinate (a thiolate) or thiosulfate ($S_2O_3^{2-}$) group could reduce the cytotoxicity of the *fac*-$[Re(CO)_3(bpy)(H_2O)]^+$ complex by converting it to a neutral or negatively charged species [27,28]. The primary goal of this study was to compare the effect of neutral ancillary thione and selone ligands on the cytotoxic properties of such complexes compared with the corresponding

Abbreviations: MMI, Methimazole (2-mercapto-1-methylimidazole); MSeI, 1-methylimidazole-2-selone; bpy, 2,2′-bipyridine; phen, 1,10-phenanthroline; dmphen, 2,9-dimethyl-1,10-phenanthroline; H_2Cys, cysteine; HSQC, Heteronuclear single quantum coherence; TD-DFT, time-dependent density functional theory; DMEM, Dulbecco's Modified Eagles Medium; PBS, Phosphate buffered saline; IC_{50}, Half-maximal inhibitory concentration.

* Corresponding author.
E-mail address: faridehj@ucalgary.ca (F. Jalilehvand).

https://doi.org/10.1016/j.jinorgbio.2022.112092
Received 28 September 2022; Received in revised form 24 November 2022; Accepted 2 December 2022
Available online 5 December 2022

fac-$[Re(CO)_3(N,N')(H_2O)]^+$ complex [12,27]. For this purpose, we chose as ligands methimazole (2-mercapto-1-methylimidazole; MMI), and its selenium analogue 1-methylimidazole-2-selone (MSeI); see Scheme 1 [30–32].

Methimazole is an antithyroid drug that prevents thyroid hormone synthesis [33,34]. Earlier studies have shown that thyroid hormones can promote tumor growth: "hypothyroidism inhibits tumor growth, while hyperthyroidism produces an opposite effect" [35]. The idea behind choosing MMI as ligand was that in case its rhenium complexes go through potential hydrolysis, the resulting species could have dual effects: the hydrated rhenium complexes would still be cytotoxic [12], while the free MMI ligands could reduce tumor growth by lowering the level of thyroid hormones. Free MSeI ligands may act as an antioxidant, saving cells from oxidative damage [31]. The cytotoxicity and inhibitory effects of a water soluble Re(I) tricarbonyl complex with a diselenoether ligand have been correlated to a significant decrease in the reactive oxygen species produced by the cancer cells [36], as well as binding to DNA bases [37].

The imidazoline-2-chalcogenone ligands are generally good σ-donors and weak π-acceptors [38]. Methimazole is predominantly present in its stable thione form in the solid state and neutral aqueous solution, while for MSeI oxidation of the tautomeric selenol to diselenide (Scheme 1) in the presence of air slowly decreases the initial selone concentration in solution [31]. In the reported structures of multinuclear rhenium(I) carbonyl complexes with methimazole, this bi-functional ligand forms a bridge between the $Re(CO)_3^+$ units [39,40].

Here, we report syntheses and structural characterizations of the triflate salts of six *fac*-$[Re(CO)_3(N,N')X]^+$ complexes (**1**–**6** in Scheme 1; X = MMI or MSeI; *N,N′* = bpy, phen or dmphen), and compare their structures and *in vitro* cytotoxic effects on the human breast cancer cell line MDA-MB-231 with those reported for the corresponding aqua and phosphine compounds (X = H_2O, PR_3). We also report their effect on the normal human embryonic kidney cell line HEK-293 T, to investigate how selective these complexes are for cancer cells.

2. Experimental section

2.1. Materials

$Re(CO)_5Cl$, 2,2′-bipyridine, 1,10-phenantroline, 2,9-dimethyl-1,10-phenanthroline, $Ag(CF_3SO_3)$, methimazole, 1-methylimidazole, *n*-butyllithium (1.6 M in hexane), selenium and $NaBH_4$ were purchased from Sigma-Aldrich and used without further purification. Toluene and tetrahydrofuran (THF) were dried over sodium and benzophenone, and then stored over 4 Å molecular sieves. Oxygen-free water was prepared by boiling distilled water and bubbling argon through it when cooling to room temperature to remove dissolved O_2. The starting materials *fac*-$[Re(CO)_3(N,N')Cl]$ (*N,N′* = bpy, phen, dmphen) [41], and the triflate salts of the aqua complexes *fac*-$[Re(CO)_3(bpy)(H_2O)]^+$ (**7***;* **Re-bpy-Aqua**), *fac*-$[Re(CO)_3(phen)(H_2O)]^+$ (**8***;* **Re-phen-Aqua**) and *fac*-$[Re(CO)_3(dmphen)(H_2O)]^+$ (**9**; **Re-dmphen-Aqua**) were prepared according to the previously published procedures [12], and characterized by measuring their unit cell dimensions and by NMR spectroscopy. A calibrated VWR Symphony SB70P pH meter was used for pH measurements.

2.2. Cell culture

The triple negative breast cancer cell line MDA-MB-231 and the human embryonic kidney cell line HEK-293 T were obtained from the American Type Culture Collection (ATCC), with frozen aliquots used within six months post thawing, and cultured with Dulbecco's Modified Eagle's Medium (DMEM; Invitrogen/Gibco), which was supplemented with heat-inactivated fetal bovine serum (10% *v*/v; Millipore Sigma),

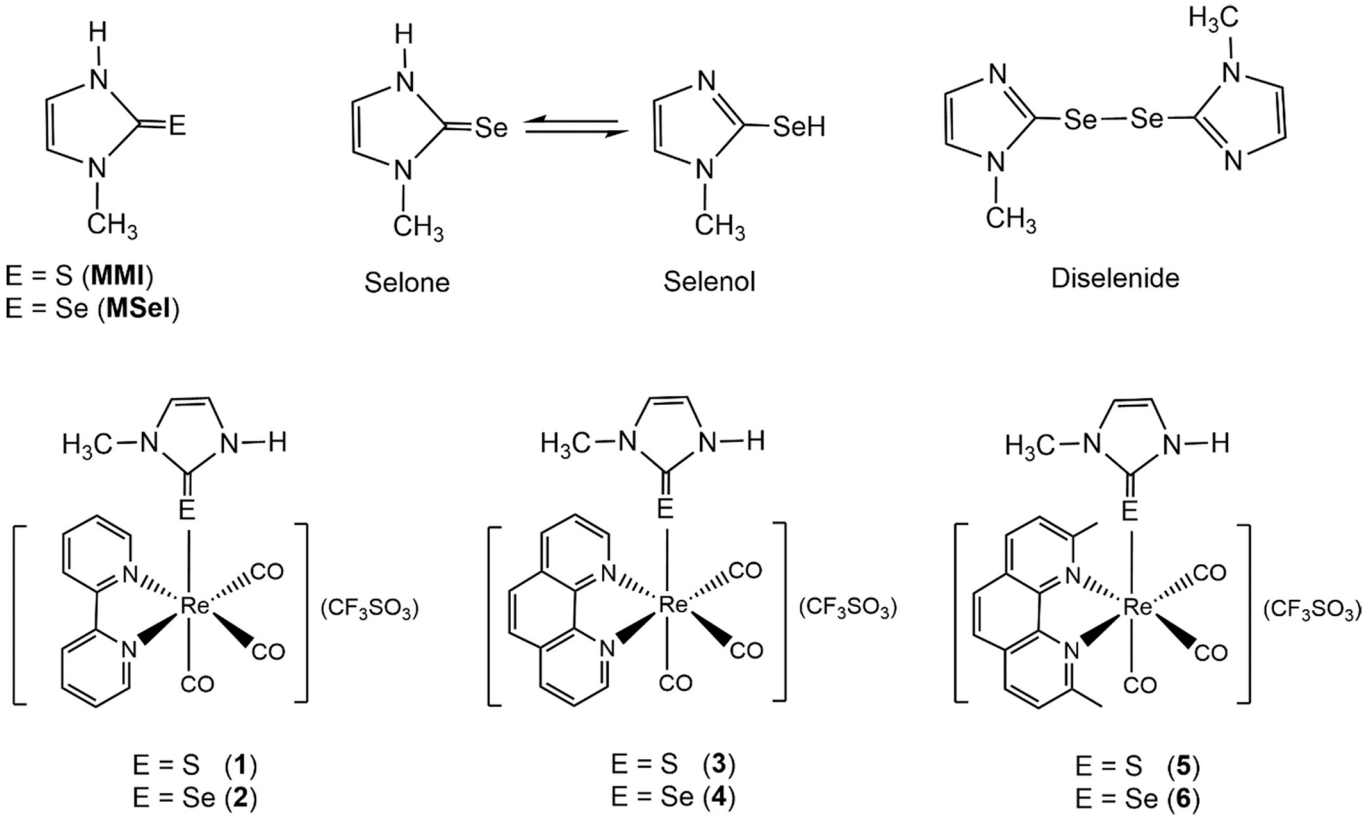

Scheme 1. *Top*) Structures of methimazole (MMI) and its selenium analogue (MSeI) (*left*); selone – selenol tautomerism for MSeI (*middle*), and its oxidation product, diselenide (*right*). *Below*) Structure of *fac*-$[Re(CO)_3(N,N')X](CF_3SO_3)$ compounds prepared in this study.

penicillin (100 units/mL; Invitrogen/Gibco), streptomycin (100 μg/mL; Invitrogen/Gibco) and L-glutamine (2 mM; Invitrogen). Cells were incubated in a humidified incubator at 37 °C with 5% CO_2 and were sub-cultured every 3–4 days for maintenance.

2.3. Syntheses

2.3.1. Synthesis of 2,2′-diselenobis(1-methylimidazole)

The diselenide (Scheme 1) and the selone ligand (MSeI) were prepared by a slight modification of a previously reported synthetic procedure [31]. 1-Methylimidazole (12.18 mmol) was added to 100 mL of freshly prepared dry deoxygenated THF under argon atmosphere. The solution was cooled to −78 °C in a dry-ice bath (acetone added) for 15 min. Cooled *n*-butyllithium (7.6 mL, 1.6 M in hexane) was added and the resulting pale yellow solution was stirred at −78 °C for 30 min. After removing the reaction flask from the dry-ice bath, the mixture was left stirring at room temperature for 2 h. This solution was transferred with a syringe to another flask (purged with argon) containing selenium (18.24 mmol) and stirred for another 12 h. The reaction mixture was then quenched with 20 mL cold deoxygenated water, and neutralized (pH 6.7) by adding 1.0 mL concentrated HCl (12 N). This process led to the formation of an orange organic layer on the top and an aqueous layer with unreacted selenium on the bottom. After decanting the organic layer, the aqueous layer was filtered to remove unreacted black solid selenium. Using a separatory funnel, the remaining product in the aqueous layer was extracted through shaking with two portions of 20 mL chloroform. All organic phases were combined, dried with anhydrous Na_2SO_4 (~ 30 mg) and filtered. The clear orange solution was rotary evaporated to dryness at 40 °C to afford the dark orange diselenide solid, which was purified by dissolving in hot chloroform and placed in the fridge to crystallize. Yield 40%. ^{1}H NMR (600 MHz, $CDCl_3$): δ_H (ppm) = 7.14 (d, J = 1.1 Hz, 2H), 7.03 (d, J = 1.1 Hz, 2H), 3.59 (s, 6H). ^{13}C NMR (600 MHz, $CDCl_3$): δ_C (ppm) = 133.6, 131.0, 124.7, 35.4 [42].

2.3.2. Synthesis of 1-methylimidazole-2-selone (MSeI)

To reduce the diselenide to selone, the above solid (4.72 mmol) was added to 100 mL water, forming a yellow-orange cloudy mixture, to which solid $NaBH_4$ (11.90 mmol) was added. After stirring the reaction mixture at room temperature over night, all diselenide dissolved. Dichloromethane (20 mL) was added to the reaction flask and after stirring, the mixture was placed in a separatory funnel to separate the organic layer. The remaining product in the top aqueous layer was further extracted with two 10 mL portions of dichloromethane. The dichloromethane extracts were combined, dried with anhydrous Na_2SO_4, and evaporated to dryness at room temperature using a rotary evaporator. The resulting bright creamy colored solid, 1-methylimidazole-2-selone (MSeI), was characterized by NMR spectroscopy and stored in a glovebox to prevent diselenide formation. Yield 20%. ^{1}H NMR (600 MHz, $CDCl_3$): δ_H (ppm) = 11.88 (br), 6.86 (d, J = 2.2 Hz, 1H), 6.82 (d, J = 2.2 Hz, 1H), 3.69 (s, 3H). ^{13}C NMR (600 MHz, $CDCl_3$): δ_C (ppm) = 152.1, 120.8, 116.5, 36.4 [42]. NMR spectra were also measured in MeOD-d^4 (Fig. S4) for comparison with those of complexes **1**–**6**.

2.4. General synthetic procedure for complexes *1*–*6*

Complex **1** was prepared by adding methimazole (MMI; 0.18 mmol) to a solution of *fac*-[$Re(CO)_3(bpy)(H_2O)$](CF_3SO_3) (0.17 mmol) in 20 mL THF, refluxing the solution for 24 h. The same product was obtained in similar yield, when the experiment was carried out at room temperature, using water as solvent. For preparing complex **2**, a solution of freshly prepared 1-methylimidazole-2-selone (MSeI; 0.16 mmol) in 5 mL deoxygenated THF was added to a solution of *fac*-[$Re(CO)_3(bpy)(H_2O)$](CF_3SO_3) (0.17 mmol in 15 mL deoxygenated THF) and refluxed for 24 h under argon atmosphere.

To prepare complexes **3**–**6**, $Re(CO)_3(N,N')Cl$ (N,N' = phen, dmphen; 0.5 mmol) was mixed with Ag(OTf) (0.5 mmol) in 40 mL THF. The mixture was refluxed for 3 h in darkness, and then filtered to remove the AgCl precipitate. The methimazole complexes **3** and **5** were obtained by adding solid MMI (0.5 mmol) to the filtrate, refluxing the mixture for 24 h. For syntheses of the selenium analogues **4** and **6**, the filtrate was degassed using a Schlenk line, then adding a freshly prepared MSeI solution (0.5 mmol in 5 mL degoxygenated THF) and refluxing the mixture for 24 h under argon.

After removing the solvent (THF) through rotary evaporation, the remaining solid was dissolved (sometimes using sonication) in 6–10 mL of a solvent to form crystals: MeOH for **2**, EtOH for **4**, and water: acetone (1:1) mixture for **3**, **5** and **6**. Depending on the solvent, two crystalline polymorphs of **1** were formed: **1a** in water: acetone (1:1) mixture, and **1b** in water. Yellow crystals, which formed through slow evaporation of the solvent at room temperature, were filtered, washed with a small amount of cold distilled water and then dried under vacuum.

*fac-[Re(CO)$_3$(bpy)(MMI)](CF$_3$SO$_3$) (**1**;* **Re-bpy-MMI***).* Elemental anal. Calcd for [$Re(CO)_3(C_{10}H_8N_2)(C_4H_6N_2S)$]($CF_3SO_3$), ($ReC_{18}H_{14}N_4O_6S_2F_3$): %C 31.35, %H 2.05, %N 8.12; Found: %C 31.34, %H 2.08, %N 7.99. Yield 74%. ^{1}H NMR (600 MHz, MeOD-d^4): δ_H (ppm) = 9.06 (d, J = 4.8 Hz, 2H), 8.58 (d, J = 8.4 Hz, 2H), 8.30 (td, J = 7.8, 1.2 Hz, 2H), 7.73 (td, J = 6.6, 1.2 Hz, 2H), 7.14 (d, J = 1.8 Hz, 1H), 6.96 (d, J = 1.8 Hz, 1H), 3.35 (s, 3H). ^{13}C NMR (151 MHz, MeOD-d^4): δ_C (ppm) = 198.0 (C11, C12), 190.1 (C13), 156.9 (C1, C1′), 154.8 (C3, C3′), 152.6 (C7), 141.6 (C5, C5′), 129.3 (C4, C4′), 125.5 (C6, C6′), 123.9 (C8), 118.7 (C9), 35.1 (C10). IR (cm^{-1}): $\tilde{\nu}_{C\equiv O}$ = 2026, 1921, 1905.

*fac-[Re(CO)$_3$(bpy)(MSeI)](CF$_3$SO$_3$) (**2**;* **Re-bpy-MSeI***).* Elemental anal. Calcd for [$Re(CO)_3(C_{10}H_8N_2)(C_4H_6N_2Se)$]($CF_3SO_3$), ($ReC_{18}H_{14}N_4O_6SeSF_3$): %C 29.35, %H 1.92, %N 7.61; Found: %C 29.30, %H 1.78, %N 7.60. Yield 30%. ^{1}H NMR (600 MHz, MeOD-d^4): δ_H (ppm) = 9.08 (d, J = 6.0 Hz, 2H), 8.53 (d, J = 8.4 Hz, 2H), 8.27 (td, J = 8.4, 1.8 Hz, 2H), 7.70 (td, J = 6.6, 1.2 Hz, 2H), 7.22 (d, J = 2.4 Hz, 1H), 7.02 (d, J = 2.4 Hz, 1H), 3.36 (s, 3H). ^{13}C NMR (151 MHz, MeOD-d^4): δ_C (ppm) = 198.1 (C11, C12), 190.0 (C13), 156.7 (C1, C1′), 154.8 (C3, C3′), 141.3 (C5, C5′), 140.1 (C7), 129.2 (C4, C4′), 125.4 (C6, C6′), 124.9 (C8), 120.5 (C9), 36.7 (C10). IR (cm^{-1}): $\tilde{\nu}_{C\equiv O}$ = 2022, 1920, 1901.

*fac-[Re(CO)$_3$(phen)(MMI)](CF$_3$SO$_3$) (**3**;* **Re-phen-MMI***).* Elemental anal. Calcd for [$Re(CO)_3(C_{12}H_8N_2)(C_4H_6N_2S)$]($CF_3SO_3$), ($ReC_{20}H_{14}N_4O_6S_2F_3$): %C, 33.66; %H, 1.98; %N, 7.85; Found: %C 33.83; %H, 1.96; %N, 7.90. Yield 93%. ^{1}H NMR (600 MHz, MeOD-d^4): δ_H (ppm) = 9.45 (dd, J = 5.1, 1.4 Hz, 2H), 8.89 (dd, J = 8.3, 1.4 Hz, 2H), 8.24 (s, 2H), 8.06 (dd, J = 8.2, 5.1 Hz, 2H), 6.88 (d, J = 2.2 Hz, 1H), 6.71 (d, J = 2.2 Hz, 1H), 3.10 (s, 3H). ^{13}C NMR (151 MHz, MeOD-d^4): δ_C (ppm) = 197.9 (C11, C12), 190.1 (C13), 155.2 (C3, C3′), 152.0 (C7), 147.6 (C1, C1′), 140.7 (C5, C5′), 132.6 (6, 6′), 129.4 (C15, C15′), 127.9 (C4, C4′), 123.5 (C8), 118.2 (C9), 34.8 (C10). IR (cm^{-1}): $\tilde{\nu}_{C\equiv O}$ = 2024, 1923, 1910.

*fac-[Re(CO)$_3$(phen)(MSeI)](CF$_3$SO$_3$) (**4**;* **Re-phen-MSeI***).* Elemental anal. Calcd for [$Re(CO)_3(C_{12}H_8N_2)(C_4H_6N_2Se)$]($CF_3SO_3$), ($ReC_{20}H_{14}N_4O_6SeSF_3$): %C, 31.58; %H, 1.86; %N, 7.37%; Found: %C 33.44; %H, 1.80; %N, 7.37. Yield: 39%. ^{1}H NMR (600 MHz, MeOD-d^4): δ_H (ppm) = 9.46 (dd, J = 5.1, 1.4 Hz, 2H), 8.86 (dd, J = 8.2, 1.3 Hz, 2H), 8.21 (s, 2H), 8.04 (dd, J = 8.2, 5.1 Hz, 2H), 6.90 (d, J = 2.4 Hz, 1H), 6.72 (d, J = 2.4 Hz, 1H), 3.07 (s, 3H). ^{13}C NMR (151 MHz, MeOD-d^4): δ_C (ppm) = 198.0 (C11, C12), 190.1 (C13), 155.3 (C3, C3′), 147.3 (C1, C1′), 140.4 (C5, C5′), 139.5 (C7), 132.5 (C6, C6′), 129.4 (C15, C15′), 127.8 (C4, C4′), 124.6 (C8), 119.9 (C9), 36.3 (C10). IR (cm^{-1}): $\tilde{\nu}_{C\equiv O}$ = 2020, 1908.

*fac-[Re(CO)$_3$(dmphen)(MMI)](CF$_3$SO$_3$) (**5**;* **Re-dmphen-MMI***).* Elemental anal. Calcd for [$Re(CO)_3(C_{14}H_{12}N_2)(C_4H_6N_2S)$]($CF_3SO_3$), ($ReC_{22}H_{18}N_4O_6S_2F_3$): %C, 35.62; %H, 2.45; %N, 7.55; Found: %C 35.47; %H, 2.42; %N, 7.74. Yield 97%. ^{1}H NMR (600 MHz, MeOD-d^4): δ_H (ppm) = 8.66 (d, J = 8.3 Hz, 2H), 8.08 (s, 2H), 8.02 (d, J = 8.3 Hz, 2H), 6.96 (d, J = 2.2 Hz, 1H), 6.85 (d, J = 2.2 Hz, 1H), 3.31 (s, 6H), 3.05 (s, 3H). ^{13}C NMR (151 MHz, MeOD-d^4): δ_C (ppm) = 197.8 (C11, C12), 189.9 (C13), 165.8 (C3, C3′), 152.1 (C7), 148.7 (C1, C1′), 140.9 (C5,

C5′), 130.9 (C6, C6′), 128.4 (C15, C15′), 128.2 (C4, C4′), 123.8 (C8), 118.6 (C9), 34.8 (C10), 31.8 (C16). IR (cm^{-1}): $\tilde{\nu}_{C\equiv O}$ = 2022, 1903.

fac-[Re(CO)$_3$(dmphen)(MSeI)](CF$_3$SO$_3$) (**6**; **Re-dmphen-MSeI**). Elemental anal. Calcd for $[Re(CO)_3(C_{14}H_{12}N_2)(C_4H_6N_2Se)](CF_3SO_3)$, ($ReC_{22}H_{18}N_4O_6SeSF_3$): %C, 33.51; %H, 2.30; %N, 7.10; Found: %C 33.86; %H, 2.37; %N, 7.16. Yield 83%. ^{1}H NMR (600 MHz, MeOD-d^4): δ_H (ppm) = 8.63 (d, *J* = 8.3 Hz, 2H), 8.05 (s, 2H), 8.00 (d, *J* = 8.3 Hz, 2H), 6.98 (d, *J* = 2.1 Hz, 1H), 6.85 (d, *J* = 2.1 Hz, 1H), 3.31 (s, 6H), 3.07 (s, 3H). ^{13}C NMR (151 MHz, MeOD-d^4): δ_C (ppm) = 198.0 (C11, C12), 189.6 (C13), 165.9 (C3, C3′), 148.7 (C1, C1′), 141.5 (C7), 140.7 (C5, C5′), 130.8 (C6, C6′), 128.4 (C15, C15′), 128.2 (C4, C4′), 124.8 (C8), 120.3 (C9), 36.4 (C10), 32.0 (C16). IR (cm^{-1}): $\tilde{\nu}_{C\equiv O}$ = 2018, 1884.

2.5. Physical measurements and methods

2.5.1. Single-crystal X-ray diffraction

Yellow single-crystals of **2** were obtained by slow evaporation of its concentrated solution in MeOH, and those of **1a**, **3**, **5** and **6** were crystallized in water: acetone (1:1) mixture. Using water as solvent led to formation of single crystals of **1b**. Crystals of **4** were not suitable for crystallography.

A suitable crystal was selected of each compound and diffraction data were obtained by means of a Bruker APEX-II CCD diffractometer at 173(2) K. Using Olex2 [43], the structures were solved with the ShelXT [44] structure solution program using Intrinsic Phasing and refined with the ShelXL [45] refinement package using Least Squares minimisation.

2.5.2. NMR spectroscopy

^{1}H, ^{13}C and HSQC 2D NMR measurements were carried out at room temperature using a Bruker Avance III 600 MHz spectrometer. ^{1}H NMR spectra of pure ligands (MMI and MSeI) in $CDCl_3$ and those of rhenium compounds in MeOD-d^4 were collected by co-adding 32 scans and internally referenced using solvent residual signals at 7.26 and 3.31 ppm, respectively [46,47]. ^{1}H NMR spectra of **1–2** were also measured in 90%H_2O (+ 10% MeOD-d^4 used as internal reference) over a period of 48 h, each time collecting 32 scans using the zgesgp pulse sequence for water suppression via application of a shaped pulse. To compare the ^{1}H NMR chemical shifts, the spectra of MMI and MSeI were also measured in MeOD-d^4. ^{13}C NMR measurements were carried out at 151 MHz at room temperature, using zgpg30 (except for **6**) or UDEFT (for **6**) pulse sequence and broadband proton decoupling, a 240 ppm sweep width, 0.5 s delay between scans (3.0 s for **6**) and 65 K data points, co-adding 2000 scans for pure ligands MMI and MSeI in $CDCl_3$ (and also in MeOD-d^4 for comparison), and Re(I) complexes **1–6**, and internally referenced using the CD_3Cl and MeOD-d^4 signals at 77.16 and 49.15 ppm, respectively [46]. The HSQC 2D NMR for **1**–**5** were obtained by co-adding 4–8 scans.

2.5.3. FT-IR spectroscopy

IR spectra were measured using an Agilent Cary 630 FT-IR with a diamond ATR accessory, averaging 8 scans for each sample.

2.5.4. UV–vis spectroscopy

Electronic absorption spectra were obtained at room temperature with a Cary 300 UV–vis double-beam spectrophotometer using a 1 cm path-length quartz cuvette, with distilled water or 2% MeOH (10% MeOH for **6**) as reference. Stock solutions (200 μM) of the rhenium (I) bipyridine complexes (**1**, **2**, **7**) were prepared in distilled water and the others in 2% MeOH (complex **6** in 10% MeOH) due to their limited solubility in water. Each sample was then further diluted using distilled water (or 2% or 10% MeOH) to 5.0×10^{-5} M, for which 3–5 scans were collected and averaged.

2.5.5. Cell viability

To determine the cytotoxicity of **1–6**, **8** and **9**, their stock solutions were prepared in complete cell culture media using DMEM: Re-bpy complexes **1** and **2** in DMEM (350 and 290 μM, respectively, for MDA-MB-231 cells and 200 μM solutions containing 2% MeOH for HEK-293 T cells), 200 μM solutions of Re-phen complexes **3**, **4** and **8** in DMEM containing 2% MeOH, and Re-dmphen complexes **5**, **6** (100 μM) and **9** (60 μM) in DMEM with 3% MeOH. Higher concentrations of **9** turned turbid after an hour. In each case, appropriate amounts of complexes **3–6**, **8** and **9** were first dissolved in 2.0 or 3.0 mL MeOH in a 100 mL volumetric flask, and then their volume was adjusted using the cell culture media. Stepwise dilution of the stock solutions using cell culture media (with 2% or 3% MeOH) led to a series of solutions with different concentrations. The procedure was repeated for all complexes **1–9** (containing 2–3% MeOH) and cisplatin prior to treating HEK-293 T cells.

MDA-MB-231 breast cancer cells were seeded in black-walled clear-bottom 96-well tissue culture plates at a density of 7500 cells/well, in a final volume of 100 μL of complete cell culture media, and cultured for ~36–48 h. Then the media was replaced with 100 μL of a freshly prepared diluted sample containing a drug (**1–6**, **8** or **9**) in varying concentrations in complete cell culture media. DMEM with 2% MeOH was used as the vehicle for the Re-phen complexes **3**, **4**, **8**, and DMEM with 3% MeOH for Re-dmphen complexes **5**, **6** and **9**. After 48 h incubation, the treatment was removed, cells were washed twice with 100 μL phosphate buffered saline (PBS) and incubated with 100 μL of 10% *v*/v solution of alamarBlue reagent (Life Technologies Corporation) in complete cell culture media; the plates were incubated for 2.5 h. The fluorescence emission at 600 nm after excitation at 570 nm was measured in a Spectramax M4 Microplate Reader. The percent control survival was calculated as (F/C) * 100, where F = fluorescence intensity of the wells of interest, and C = average fluorescence intensity of the wells containing cells incubated with complete cell culture media. The graphs were created using Graph Pad Prism software (version 9.3.0). In order to calculate the half-inhibitory concentration (IC_{50}), the percent control survival vs logarithm of drug concentration graphs was adjusted to a logarithmic curve. The percent viability data are the mean of three (for **1** and **2**) or six (for **3–6**, **8**, **9**) experimental replicates per concentration, and three independent experiments.

The above procedure was repeated for the HEK-293 T cells: DMEM with 2% MeOH was used as the vehicle for the Re-bpy and Re-phen complexes (**1–4**, **7**, **8**), and DMEM with 3% MeOH for Re-dmphen complexes (**5**, **6**, **9**). For cisplatin, DMEM was added as the vehicle. The cells were incubated with each drug for 48 h. The cell viability (%) data are representative of three independent experiments, each with six replicates.

3. Results and discussion

Reactions of diimine Re(I) tricarbonyl compounds, *fac*-[Re(CO)$_3$(*N*,*N*′)X](CF$_3$SO$_3$), (*N*,*N*′ = bpy, phen, dmphen; X = H_2O or THF), with methimazole and its selenium analogue in THF solution led to a series of air-stable Re(I) complexes coordinated to these imidazoline-2-thione/selone ligands, which were characterized by X-ray crystallography, elemental analysis, multinuclear (^{1}H, ^{13}C) and 2D NMR, UV–vis and IR spectroscopic techniques. Scheme 2 displays the synthetic procedure for the water soluble compound *fac*-[Re(bpy)(CO)$_3$(MSeI)](CF$_3$SO$_3$) (**2**), which was crystallized from its methanol solution.

3.1. X-ray crystallography

Crystallization of the water soluble methimazole compound, *fac*-[Re(bpy)(CO)$_3$(MMI)](CF$_3$SO$_3$) (**Re-bpy-MMI**; **1**), led depending on the solvent used (see the *Experimental Section*), to two polymorphs **1a** and **1b**. Evidently, their energy difference must be small, with the MMI ring stacked nearly above the bipyridine ligand in **1a**, but in **1b** adopting the opposite direction away from bipyridine closer to the equatorial carbonyl ligands (Fig. 1). Crystal data, structural refinements, as well as selected bond distances and angles for **1a**, **1b**, *fac*-[Re(CO)$_3$(bpy)(MSeI)](CF$_3$SO$_3$) (**2**; **Re-bpy-MSeI**), *fac*-[Re(CO)$_3$(phen)(MMI)](CF$_3$SO$_3$) (**3**;

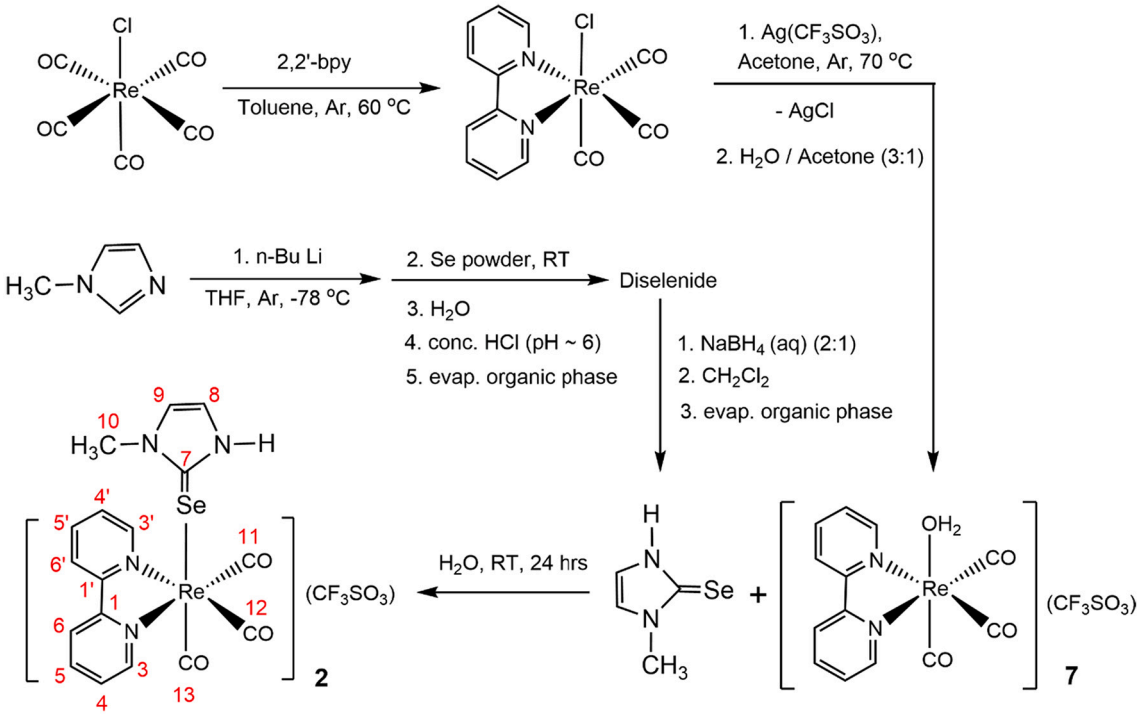

Scheme 2. Synthetic procedure for the *fac*-[Re(CO)$_3$(bpy)(MSeI)](CF$_3$SO$_3$) compound (**2**). The numbers in red refer to the carbon atoms associated with its crystal structure and the ^{13}C NMR signals described in the "*Experimental Section*".

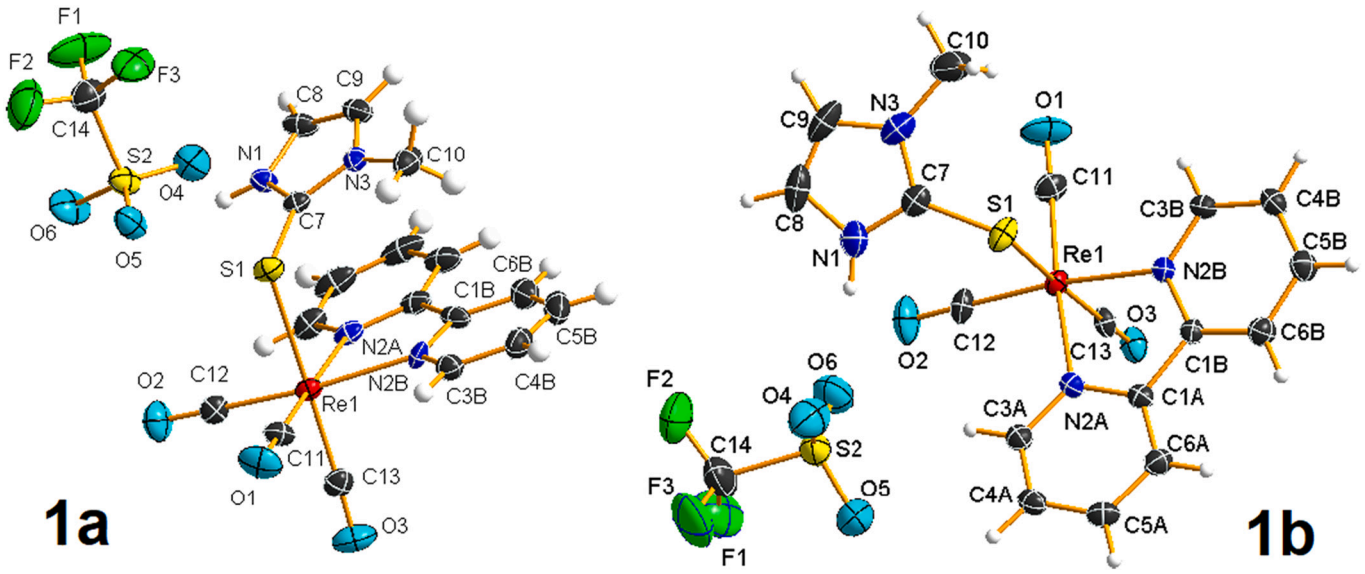

Fig. 1. Two polymorphs of *fac*-[Re(bpy)(CO)$_3$(MMI)](CF$_3$SO$_3$): **1a** crystallized from water: acetone (1:1), **1b** from water. Only one of the two ion-pairs in the asymmetric unit of **1b** is shown here. Thermal ellipsoids are shown at 50% probability level.

Re-phen-MMI) and *fac*-[Re(CO)$_3$(dmphen)(MSeI)](CF$_3$SO$_3$) (**6**; **Re-dmphen-MSeI**) are reported in Tables S1 and S2, with crystal structures of **2, 3** and **6** displayed in Fig. 2. The crystal structure of *fac*-[Re(CO)$_3$(dmphen)(MMI)](CF$_3$SO$_3$) (**5**; **Re-dmphen-MMI**) was disordered, with two slightly twisted orientations for the Re(I) complex (Fig. S1).

The crystal structures of **1a** and **2** are isomorphous with the same space group. In all other crystal structures, the orientations of the imidazoline rings are different. Still one of the nitrogen atoms in the imidazoline ring (N1) forms a rather strong hydrogen-bond to the triflate ions with N1—H….O about 2.8–2.9 Å. Such hydrogen bond ability would promote solubility of the complexes in the aqueous solution.

In these structures, methimazole (MMI) and its selenium analogue (MSeI) appear in their thione and selone forms, respectively. The C7—S bond distances in the coordinated MMI in **1a**, **1b** and **3** are all longer (Table S2) than the C—S distances in the pure MMI ligand, 1.682(2) and 1.686(2) Å [48]. Similar elongation is observed for the C7—Se distance of the Re(I) bound selone group in **2** and **6** relative to the corresponding C—Se distance in the pure MSeI ligand, 1.849(3) Å [42]. This observation is probably due to π-back donation from the filled Re(I) t_{2g} orbitals to π* (C=S/Se), making the bond somewhat weaker and longer.

The Re—CO$_{axial}$ bond distances in the MMI/MSeI complexes **1a**, **1b** and **2** (Re—C $_{axial}$ = 1.91–1.92 Å, Table S2) are longer for the CO ligands

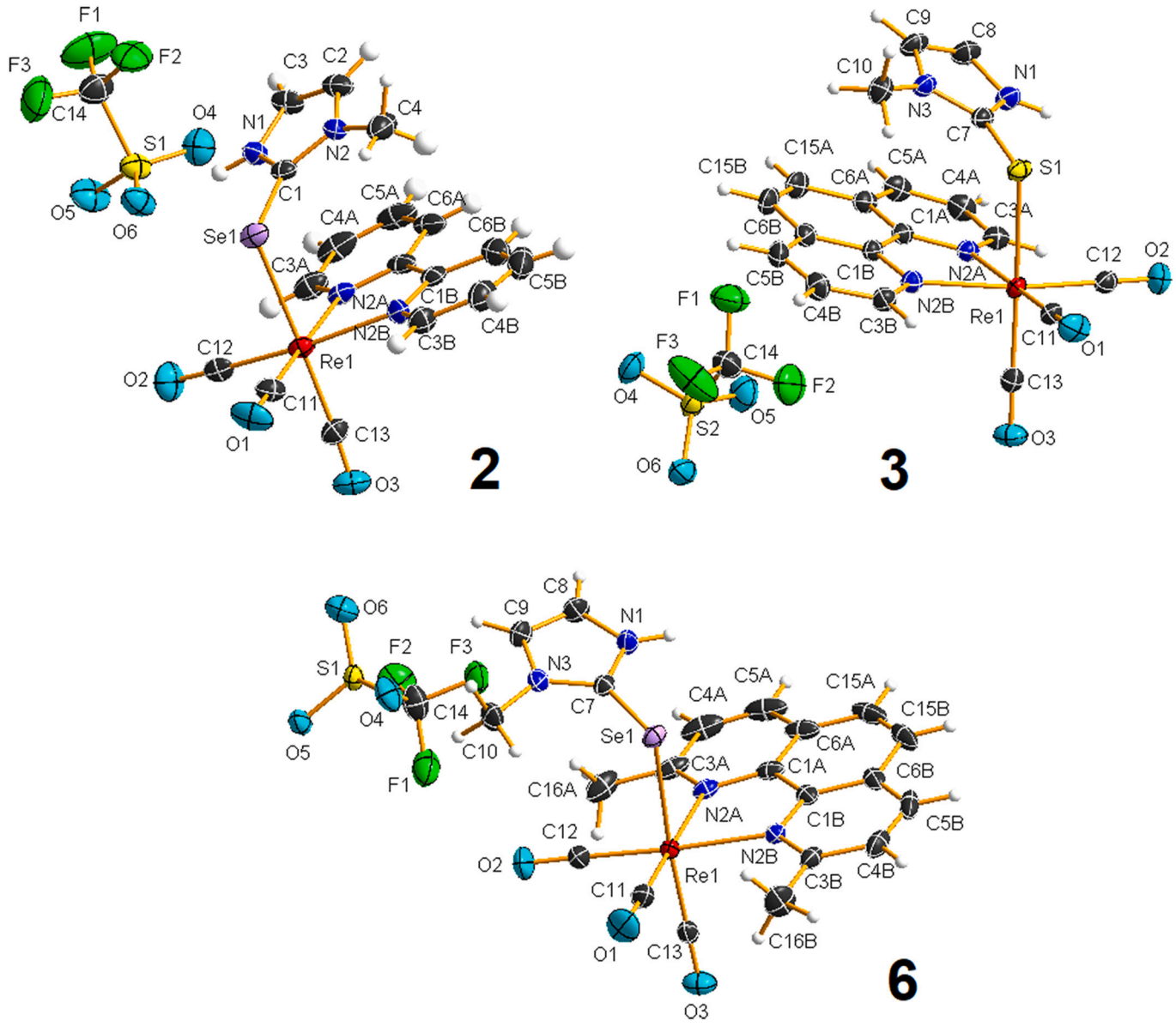

Fig. 2. Crystal structures of *fac*-[Re(CO)$_3$(bpy)(MSeI)](CF$_3$SO$_3$) (**2**), *fac*-[Re(CO)$_3$(phen)(MMI)](CF$_3$SO$_3$) (**3**) and *fac*-[Re(CO)$_3$(dmphen)(MSeI)](CF$_3$SO$_3$) (**6**). Disordered components have been removed for clarity.

trans to the thione/selone groups than that for the CO ligand *trans* to the aqua ligand in the crystal structure of *fac*-[Re(CO)$_3$(bpy)(H$_2$O)](CF$_3$SO$_3$) (**7**; Re—C $_{axial}$ = 1.882(10) Å) [49]. Similar elongation is observed when comparing the influence of aqua and MMI ligands on the Re—CO$_{axial}$ distances in *fac*-[Re(CO)$_3$(phen)(H$_2$O)](CF$_3$SO$_3$) (**8**) and *fac*-[Re(CO)$_3$(phen)(MMI)](CF$_3$SO$_3$) (**3**) with Re—C$_{axial}$ 1.898(7) Å and 1.923(2) Å, respectively [49]. The elongation is consistent with the stronger sigma bond formed between the soft Re(I) ion and the soft S/Se donor atom in the MMI and MSeI ligands, than with the aqua ligand, leading to stronger *trans* influence on the Re—CO$_{axial}$ bonds.

The Re—S bond lengths in the Re-MMI complexes **1a**, **1b** and **3**, which vary over a narrow range 2.516(1) ~ 2.545(2) Å, and the Re—Se bond distance of 2.650(1) Å in the Re-MSeI complexes **2** and **6** are comparable with the average Re—S and Re—Se distances 2.516(2) Å and 2.643(3) in the [Re(CO)$_3${HB(SIm^{Me})$_3$}] and [Re(CO)$_3${HB(SeIm^{Mes})$_3$}] complexes, respectively, where {HB(SIm^{Me})$_3$} = tris(2-mercapto-1-methylimidazolyl)hydroborate and {HB(SeIm^{Mes})$_3$} = tris(2-seleno-1-mesitylimidazolyl)hydroborate [50,51].

In the previously reported crystal structures for similar complexes with phosphine ligands, [Re(CO)$_3$(bpy)(PR$_3$)]$^+$ [16], the average Re—P bonds (2.43–2.44 Å) are about 0.1–0.2 Å shorter than the corresponding Re—S and Re—Se distances in **1a/1b** and **2**, respectively. Furthermore, the Re—CO$_{axial}$ bonds (1.96 Å) are slightly longer than those in **1a/1b** and **2** (1.91–1.92 Å), implying that the phosphine ligands have even stronger *trans*-influence than MMI and MSeI. An increasing σ-donor and π-acceptor ability of the PR$_3$ ligands with π-competition for the same metal orbitals is consistent with a weaker, longer *trans* Re—CO$_{axial}$ bond [15].

3.2. Vibrational spectroscopy

The characteristic C ≡ O vibrational stretching bands that occur in the 2040–1890 cm^{-1} range for the Re(I) aqua complexes **7**–**9**, generally appear at lower frequencies for the complexes **1a** – **6** (Fig. S2 and Table S3). Such shift indicates weaker C ≡ O bonds, probably because of increased π-back-donation from the electron-rich Re(I) ions bound to the thione/selone ligands (relative to H$_2$O) to π* of the carbonyl group [50,52].

3.3. NMR spectroscopy

The ^{1}H and ^{13}C NMR signals for C8—H and C9—H in Re(I)-bound MMI and MSeI in **1** and **2** showed a slight downfield shift ($\Delta\delta_H < 0.2$ ppm, $\Delta\delta_C \leq 3$ ppm) relative to those of the pure ligands (see Table S4, Figs. S3–S6), since transfer of electron density from the coordinated MMI/ MSeI ligands to the Re(I) ion has a deshielding effect on both the H and C atoms. Similar relative ^{13}C downfield shifts were observed for the ligands' C8 and C9 atoms in the Re-phen and Re-dmphen complexes **3**–**6**. However, the C8—H and C9—H proton NMR resonances in the Re-phen complexes **3** and **4** were somewhat shielded relative to those of pure MMI and MSeI ligands, which could be due to stacking of the MMI/ MSeI ligands above the phen ring, as shown in the crystal structure of the Re-phen-MMI complex (**3**) in Fig. 2.

The ^{13}C NMR signal for the carbene C7 atom (C—S/Se) of the pure ligands MIM (δ_C = 161.6 ppm) and MSeI (δ_C = 152.3 ppm) showed significant upfield shift ($\Delta\delta_C$ 9–13 ppm) in the ^{13}C NMR spectra of the Re (I) complexes **1**–**6**; see Figs. S3–S10 and Table S4. Such an upfield shift of the ^{13}C signal has been attributed to decreasing π-acceptance character of the carbene C atom upon coordination [53]. In free *N*-heterocyclic carbenes (NHCs), promotion of an electron from the σ(NHC lone pair) to the p_π acceptor orbital on the carbene C atom contributes to the paramagnetic shielding term, leading to a downfield shift of carbene δ_C [54]. In imidazoline-2-chalcogenones such as MSeI, the π backdonation Se ($4p_y$) → Se-C(π*) that contributes to a paramagnetic shielding term is decreased upon Se($4p_y$) → metal coordination, resulting in an upfield shift of the carbene δ_C [55,56].

3.4. Electronic absorption spectroscopy

The UV–vis absorption spectra of the Re(I) complexes **1**–**9** displayed in Fig. 3 show that the band at 345 nm for the Re-bpy-Aqua complex (**7**) shifts to higher wavelengths (red-shift) to 362 and 367 nm for Re-bpy-MMI (**1**) and Re-bpy-MSeI (**2**), respectively. These electronic transitions are attributed to a metal-to-ligand charge transfer (MLCT) d(Re) → π*(bpy); see the Computational Studies in the Supplementary Data. Also, the intensity of the bands at 245 and ~ 300 nm increases noticeably for **1** and **2**, relative to **7**. The spectra of Re-MMI complexes **3** and **5** show two distinct features in the 255–275 nm range.

These complexes were stable in aqueous (or 2% MeOH) solutions when irradiated with UV-A light (λ = 365 nm) for 2 h (Fig. S12), otherwise observable changes in the UV–vis spectra would be expected as a result of changes in the Re(I) coordination geometry [16]. The minor changes observed in the UV–vis spectra in Fig. S12 are due to photo-bleaching.

3.5. Ligand exchange in aqueous media

To check the stability of the complexes, and the possibility of MMI/ MSeI ligand exchange with water molecules in aqueous media, ^{1}H NMR spectra of the water soluble Re-bpy-MMI (**1**) and Re-bpy-MSeI (**2**) complexes were measured at different time intervals over a 48 h period in 90% H_2O (+ 10% MeOD-d^4 used as internal reference). As shown in Fig. 4, the Re(I) methimazole complex (**1**) is rather stable in aqueous solution with ~18% of the complex being hydrolyzed after 24 h and ~ 27% after 48 h (based on the relative peak integrals in the 9.1–9.2 ppm region); peaks related to the hydrolyzed species are marked with (*). The ligand exchange is much slower for the MSeI ligand in **2**, as shown in Fig. S11, with only ~10% of the complex hydrolyzed after 24 h. Based on these results, limited amount of free ligand from the hydrolysis process is released in the aqueous media at room temperature.

3.6. Cytotoxicity

The effect of the Re(I) complexes **1–6** on cell viability was determined by testing varying concentrations of these complexes in the human breast cancer cells (MDA-MB-231) and in the human embryonic kidney cells (HEK-293 T), checking the selectivity of these complexes towards cancerous vs. normal cells. The results are presented in Fig. 5, S15 and Table 1.

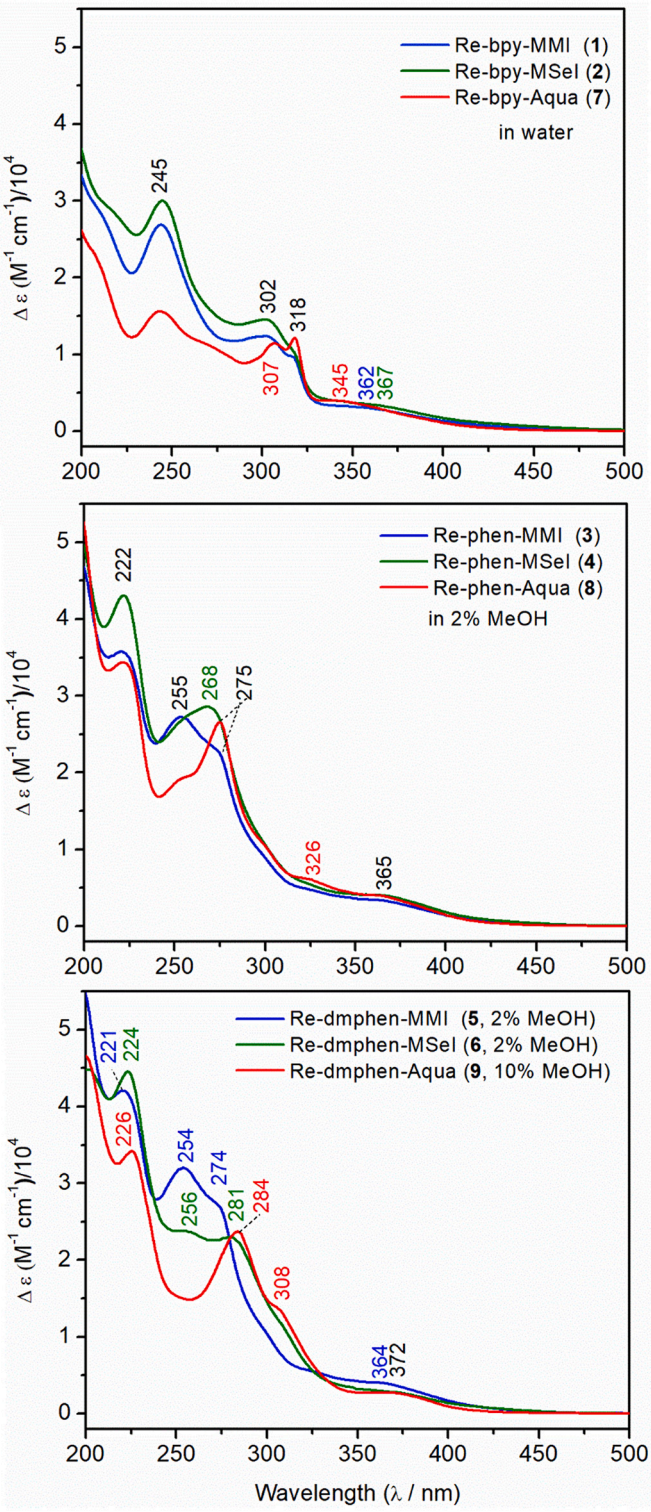

Fig. 3. UV–vis absorption spectra of air-equilibrated aqueous media (5.0×10^{-5} M) of *fac*-[Re(*N,N'*)$(CO)_3$X](CF_3SO_3) compounds: (*top*) *N,N'* = bpy, X = MMI (**1**), MSeI (**2**), H_2O (**7**); (*middle*) *N,N'* = phen, X = MMI (**3**), MSeI (**4**), H_2O (**8**); (*below*) *N,N'* = dmphen, X = MMI (**5**), MSeI (**6**), H_2O (**9**). Common absorption maxima are shown in black.

Complexes **1** and **2** with the MMI/MSeI ligands have significantly

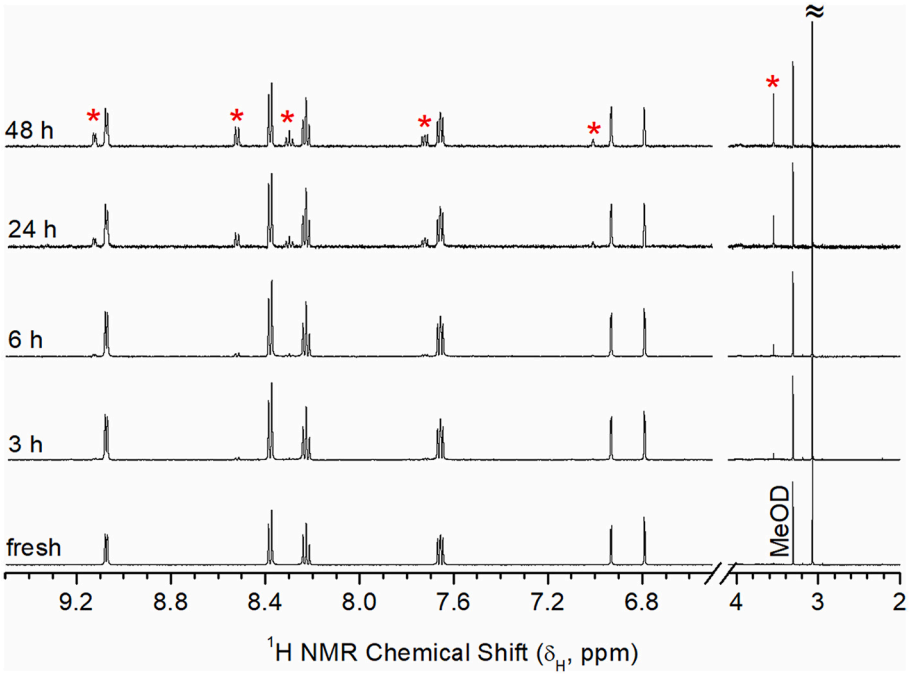

Fig. 4. ^{1}H NMR spectra of *fac*-[Re(CO)$_3$(bpy)(MMI)](CF$_3$SO$_3$) (**1**; Re-bpy-MMI) in (90% H_2O + 10% MeOD-d^4) over 48 h. Peaks shown with (*) are related to the hydrolysis products: the Re-bpy-Aqua (**7**) complex and the free MMI ligand.

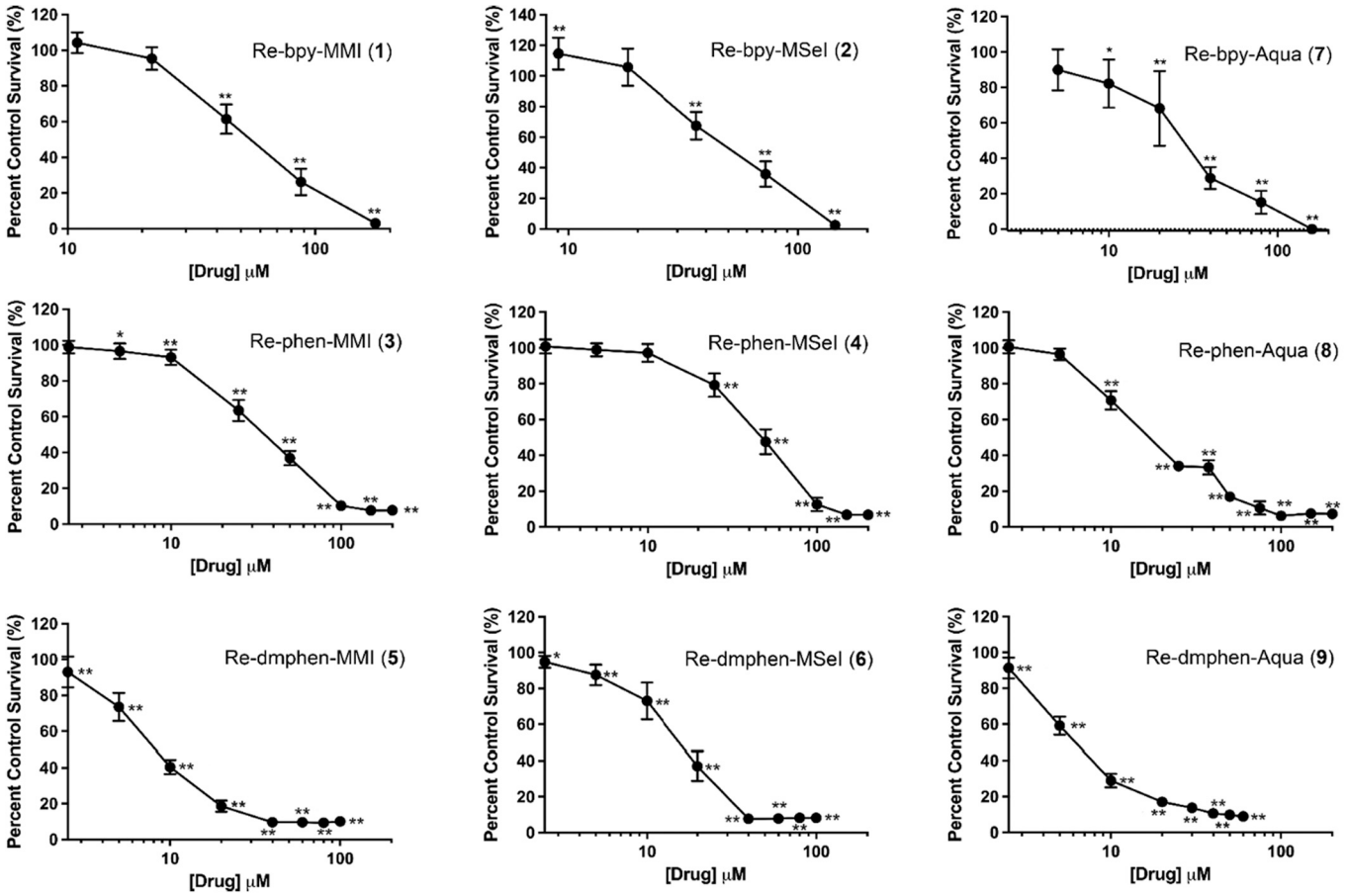

Fig. 5. Cytotoxicity of the Re(I) complexes **1**–**9** in the human breast cancer cells (MDA-MB 231). Cells were incubated with each compound for 48 h. The error bars represent the standard deviation. The data were analyzed using a one-way ANOVA, followed by a Dunnett's Test; the asterisks represent significant differences in comparison to the control group (no treatment), *: $p < 0.05$, **: $p < 0.01$. The data represent three independent experiments, each with three (for **1** and **2**), six (for **3**–**6**, **8**, **9**) or nine (for **7** - from Ref [27]) experimental replicates.

higher cytotoxicity towards MDA-MB-231 cells (Table 1) in comparison with the two Re(I) complexes containing X = S-donor ligands that were previously studied in our group, i.e. the neutral cysteinate complex, *fac*-[$Re(CO)_3$(bpy)(HCys)], and the anionic *fac*-[$Re(CO)_3$(bpy)(S_2O_3)]$^-$ [27,28]. The reason is probably due to the cationic nature of these species and their higher cell membrane permeability that leads to higher cellular uptake through passive diffusion [57–59].

Comparing the cytotoxicity of MMI vs. MSeI rhenium(I) complexes, the Re-MMI complexes **3** and **5** were somewhat more toxic with lower IC_{50} relative to their selenium analogues **4** and **6**, respectively, or with very similar cytotoxicity (**1** and **2** towards breast cancer cells). Of the three sets of diimine complexes tested in this study, the Re-dmphen complexes (**5**, **6** and **9**) displayed the highest toxicity. In each set, the aqua complexes *fac*-[$Re(CO)_3$(*N,N′*)X]$^+$ (X = H_2O; **7**–**9**) were generally more toxic towards the breast cancer cells than the corresponding X = MMI/ MSeI complexes (**1**–**6**) with the lowest IC_{50} = 6.0 ± 0.1 μM for *fac*-[$Re(CO)_3$(dmphen)(H_2O)]$^+$ (**9**) (see Table 1). This value is comparable to a range of reported IC_{50} values for this complex, tested in several cell lines (other than MDA-MB 231), varying from 0.92 ± 0.20 to 6.7 ± 4.9 (cell exposure time = 72 h) [12]. Remarkably, among the Re-dmphen complexes, the Re-dmphen-Aqua (**9**) was the least toxic one towards HEK-293 T cells (IC_{50} = 20.0 ± 0.4 μM), showing three times higher selectivity towards MDA-MB-231 breast cancer cells. The other Re-aqua complexes (**7** and **8**) as well as the Re-bpy complexes **1** and **2** were more toxic and selective towards MDA-MB-231 than HEK-293 T cells, although to a lesser extent than **9**. The Re-phen-MMI (**3**) and Re-phen-MSeI (**4**) complexes were found to be equally or more toxic towards HEK-293 T human embryonic kidney cells, with Re-dmphen-MMI (**5**) being the most toxic.

The mechanism of action of these complexes is unknown. The ability of **1** and **2** in generating $^1O_2$ was tested using a direct detection method as described earlier [27], giving negative results. It is unlikely that these Re-MMI/MSeI complexes become activated through hydrolysis [60]; as discussed in Section 3.5, <10–20% of complexes **1** and **2** hydrolyzed over a 24 h period.

Complexes **1**–**6** with a thione/ selone donor ligand seem to be more toxic ($IC_{50} \leq 55$ μM for MDA-MB-231 cells) than phosphine complexes *fac*-[$Re(CO)_3$(*N,N′*)(PR_3)]$^+$ with similar diimine ligands [16]. However, these phosphine complexes exhibit photo-cytotoxicty, i.e. they have the advantage of having minimal toxicity in the dark ($IC_{50} > 200$ μM in HeLa cells), but become highly toxic upon irradiation with 365 nm light – an ideal case for selectively targeting cancer cells. Note that irradiation of complexes **1**–**5** with 365 nm light did not cause any changes in their UV–vis. Spectra (*see above*).

4. Conclusion

Two series of diimine tricarbonyl rhenium(I) complexes with the soft and polarizable thione (methimazole; MMI) or selone (1-methyl-imidazole-2-selone; MSeI) ligands were reported for the first time: *fac*-[$Re(CO)_3$(*N,N′*)(MMI)]$^+$ and *fac*-[$Re(CO)_3$(*N,N′*)(MSeI)]$^+$, where *N,N′* = bpy, phen and dmphen. Their cytotoxicity on the human breast cancer (MDA-MB-231) and the human embryonic kidney (HEK-293 T) cell lines were determined *in vitro*. The highest toxicity was found for *fac*-[$Re(CO)_3$(dmphen)(MMI)]$^+$ (**5**) with IC_{50} = 8.0 ± 0.2 μM (for MDA-MB-231), similar to that of the corresponding aqua complex, *fac*-[$Re(CO)_3$(dmphen)(H_2O)]$^+$ with IC_{50} = 6.0 ± 0.1 μM; the latter had three times higher selectivity towards the cancer cells. Least toxic were the water soluble *fac*-[$Re(CO)_3$(bpy)(MMI / MSeI)]$^+$ complexes (**1**, **2**; IC_{50} = 55 ± 3 μM for the cancer cells and 72–80 μM for the normal cells).

These thione/ selone Re(I) complexes were significantly more cytotoxic ($IC_{50} \leq 55$ μM) than the corresponding *fac*-[$Re(CO)_3$(*N,N′*)(PR_3)]$^+$ complexes with a phosphine ligand that display little to no toxicity in the dark ($IC_{50} > 200$ μM in HeLa cells) [16]. However, unlike the phosphine complexes, they were stable in aqueous media and did not release a CO ligand upon irradiation with 365 nm light, and are therefore not candidates as photo-activated anticancer agents.

Table 1
IC_{50} values of the compounds in the human breast cancer cell line MDA-MB 231 and the human embryonic kidney cell line HEK-293 T after 48 h treatment[a].

Compound	MDA-MB-231 IC_{50} (μM)	HEK-293 T IC_{50} (μM)
cisplatin	11 ± 2[b]	23 ± 1
fac-$Re(CO)_3$(bpy)(HCys)	> 100[b]	
Na[*fac*-$Re(CO)_3$(bpy)(S_2O_3)]	> 100[c]	
Re-bpy-MMI (**1**)	55 ± 2	72 ± 2
Re-bpy-MSeI (**2**)	55 ± 3	80 ± 2
Re-bpy-Aqua (**7**)	26 ± 3[b]	45 ± 1
Re-phen-MMI (**3**)	35 ± 1	35 ± 1
Re-phen-MSeI (**4**)	45 ± 1	38 ± 1
Re-phen-Aqua (**8**)	19.0 ± 0.7	31.0 ± 0.8
Re-dmphen-MMI (**5**)	8.0 ± 0.2	11.0 ± 0.2
Re-dmphen-MSeI (**6**)	14.0 ± 0.4	15.0 ± 0.4
Re-dmphen-Aqua (**9**)	6.0 ± 0.1	20.0 ± 0.4

[a] The values given as IC_{50} ± standard deviation represent three independent experiments, each with six replicates for the HEK-293 T cell line, and for the MDA-MB-231 cell line, each experiment with three (for **1** and **2**), six (for **3**–**6**, **8**, **9**) or nine (for cisplatin and **7**) replicates.
[b] Ref [27].
[c] Ref [28].

Crystallography data

CCDC 2201417–2201422 contain the supplementary crystallographic data for this paper. These data can be obtained free of charge via www.ccdc.cam.ac.uk/data_request/cif, or by emailing data_request@ccdc.cam.ac.uk, or by contacting The Cambridge Crystallographic Data Centre, 12 Union Road, Cambridge CB2 1EZ, UK; fax: +441,223 336,033.

Author statement

All authors contributed by performing the experiments and/or data collection/ data analyses, discussed the results and commented on the manuscript. F.J. and V.B. wrote the manuscript with input from all other authors.

Declaration of Competing Interest

The authors declare that they have no known competing financial interests or personal relationships that could have appeared to influence the work reported in this paper.

Data availability

Data will be made available on request.

Acknowledgements

This work was financially supported by the Natural Sciences and Engineering Research Council of Canada (NSERC) funding reference numbers RGPIN 2016-04546 and 2022-02996 (FJ), Canada Foundation for Innovation (Grant no. 9479) and the Province of Alberta - Department of Innovation and Science (FJ), University of Calgary SEED Grant no. 1054307 (FJ), and the Alberta Cancer Foundation Grant no. 27246 (CS). Theoretical calculations were performed using the computer resources provided by WestGrid (www.westgrid.ca) and Digital Research Alliance of Canada (alliancecan.ca). We are grateful to Professor Belinda Heyne's group for testing the ability of **1** and **2** in generating $^1O_2$. V.B. acknowledges NSERC Undergraduate Student Research Award (USRA), and is grateful to Mr. Miles Capper for providing a portion of the *fac*-[$Re(CO)_3$(bpy)(H_2O)](CF_3SO_3) complex (**7**) used for syntheses of **1** and **2**.

Appendix A. Supplementary data

Supplementary data to this article can be found online at https://doi.org/10.1016/j.jinorgbio.2022.112092.

References

[1] K.A. Grice, C.P. Kubiak, in: M. Aresta, R. van Eldik (Eds.), Advances in Inorganic Chemistry, Academic Press, 2014, pp. 163–188.
[2] J. Agarwal, E. Fujita, H.F. Schaefer, J.T. Muckerman, J. Am. Chem. Soc. 134 (2012) 5180–5186.
[3] S. Hostachy, C. Policar, N. Delsuc, Coord. Chem. Rev. 351 (2017) 172–188.
[4] E.B. Bauer, A.A. Haase, R.M. Reich, D.C. Crans, F.E. Kühn, Coord. Chem. Rev. 393 (2019) 79–117.
[5] A. Leonidova, G. Gasser, ACS Chem. Biol. 9 (2014) 2180–2193.
[6] K. Schindler, F. Zobi, Molecules 27 (2022), 1-25, 539, https://www.mdpi.com/1420-3049/27/2/539.
[7] P. Collery, D. Desmaele, V. Vijaykumar, Curr. Pharm. Des. 25 (2019) 3306–3322. https://pubmed.ncbi.nlm.nih.gov/31475892/.
[8] C.C. Konkankit, J. Lovett, H.H. Harris, J.J. Wilson, Chem. Commun. 56 (2020) 6515–6518.
[9] J.L. Wedding, H.H. Harris, C.A. Bader, S.E. Plush, R. Mak, M. Massi, D.A. Brooks, B. Lai, S. Vogt, M.V. Werrett, Metallomics 9 (2017) 382–390. https://pubs.rsc.org/en/content/articlelanding/2017/mt/c6mt00243a.
[10] K. Talukdar, S. Sinha Roy, E. Amatya, E.A. Sleeper, P. Le Magueres, J.W. Jurss, Inorg. Chem. 59 (2020) 6087–6099.
[11] R.-R. Ye, C.-P. Tan, M.-H. Chen, L. Hao, L.-N. Ji, Z.-W. Mao, Chem. Eur. J. 22 (2016) 7800–7809.
[12] K.M. Knopf, B.L. Murphy, S.N. MacMillan, J.M. Baskin, M.P. Barr, E. Boros, J. J. Wilson, J. Am. Chem. Soc. 139 (2017) 14302–14314.
[13] C.C. Konkankit, A.P. King, K.M. Knopf, T.L. Southard, J.J. Wilson, ACS Med. Chem. Lett. 10 (2019) 822–827.
[14] L.C.-C. Lee, K.-K. Leung, K.K.-W. Lo, Dalton Trans. 46 (2017) 16357–16380. https://pubs.rsc.org/en/content/articlelanding/2017/dt/c7dt03465b.
[15] I. Chakraborty, J. Jimenez, W.M.C. Sameera, M. Kato, P.K. Mascharak, Inorg. Chem. 56 (2017) 2863–2873.
[16] S.C. Marker, S.N. MacMillan, W.R. Zipfel, Z. Li, P.C. Ford, J.J. Wilson, Inorg. Chem. 57 (2018) 1311–1331.
[17] K. Koike, N. Okoshi, H. Hori, K. Takeuchi, O. Ishitani, H. Tsubaki, I.P. Clark, M. W. George, F.P.A. Johnson, J.J. Turner, J. Am. Chem. Soc. 124 (2002) 11448–11455. https://pubs.acs.org/doi/10.1021/ja017032m.
[18] E. Hevia, J. Pérez, L. Riera, V. Riera, I. del Río, S. García-Granda, D. Miguel, Chem. Eur. J. 8 (2002) 4510–4521. https://chemistry-europe.onlinelibrary.wiley.com/doi/10.1002/1521-3765(20021004)8:19%3C4510::AID-CHEM4510%3E3.0.CO;2-L.
[19] D.C. Gerbino, E. Hevia, D. Morales, M.E.N. Clemente, J. Pérez, L. Riera, V. Riera, D. Miguel, Chem. Commun. (2003) 328–329. https://pubs.rsc.org/en/content/articlelanding/2003/cc/b210860g.
[20] L. Cuesta, D.C. Gerbino, E. Hevia, D. Morales, M.E. Navarro Clemente, J. Pérez, L. Riera, V. Riera, D. Miguel, I. del Río, S. García-Granda, Chem. Eur. J. 10 (2004) 1765–1777. https://chemistry-europe.onlinelibrary.wiley.com/doi/10.1002/chem.200305577.
[21] L. Cuesta, M.A. Huertos, D. Morales, J. Pérez, L. Riera, V. Riera, D. Miguel, A. Menéndez-Velázquez, S. García-Granda, Inorg. Chem. 46 (2007) 2836–2845.
[22] S.E. Kabir, J. Alam, S. Ghosh, K. Kundu, G. Hogarth, D.A. Tocher, G.M.G. Hossain, H.W. Roesky, Dalton Trans. (2009) 4458–4467.
[23] R.F. Semeniuc, T.J. Reamer, J.P. Blitz, K.A. Wheeler, M.D. Smith, Inorg. Chem. 49 (2010) 2624–2629.
[24] R. Arévalo, J. Pérez, L. Riera, Inorg. Chem. 52 (2013) 6785–6787.
[25] V. Fernández-Moreira, H. Sastre-Martín, Inorg. Chim. Acta 460 (2017) 127–133.
[26] M. He, H.V. Ching, C. Policar, H.C. Bertrand, New J. Chem. 42 (2018) 11312–11323. https://pubs.rsc.org/en/content/articlelanding/2018/nj/c8nj01960f.
[27] M.S. Capper, A. Enriquez Garcia, N. Macia, B. Lai, J.-B. Lin, M. Nomura, A. Alihosseinzadeh, S. Ponnurangam, B. Heyne, C.S. Shemanko, F. Jalilehvand, J. Biol. Inorg. Chem. 25 (2020) 759–776.
[28] M.S. Capper, A. Enriquez Garcia, B. Lai, O.B. Wang, B.S. Gelfand, C.S. Shemanko, F. Jalilehvand, Dalton Trans. 50 (2021) 5968–5977.
[29] A. Gómez, G. Jara, E. Flores, T. Maldonado, F. Godoy, M. Muñoz-Osses, A. Vega, R. Mera, C. Silva, J. Pavez, New J. Chem. 44 (2020) 14171–14179.
[30] G. Roy, G. Mugesh, Bioinorg. Chem. Appl. (2006) 1–9, 23214, https://www.hindawi.com/journals/bca/2006/023214/.
[31] G. Roy, G. Mugesh, J. Am. Chem. Soc. 127 (2005) 15207–15217.
[32] K.P. Bhabak, G. Mugesh, Chem. Eur. J. 16 (2010) 1175–1185.
[33] D.S. Cooper, N. Engl. J. Med. 352 (2005) 905–917. https://www.nejm.org/doi/full/10.1056/nejmra042972.
[34] F. Isaia, M.C. Aragoni, M. Arca, F. Demartin, F.A. Devillanova, G. Floris, A. Garau, M.B. Hursthouse, V. Lippolis, R. Medda, F. Oppo, M. Pira, G. Verani, J. Med. Chem. 51 (2008) 4050–4053.
[35] E. Krashin, A. Piekiełko-Witkowska, M. Ellis, O. Ashur-Fabian, Front. Endocrinol. 10 (2019), 1-23, 59, https://www.frontiersin.org/articles/10.3389/fendo.2019.00059/full.
[36] P. Collery, V. Veena, A. Harikrishnan, D. Desmaele, Investig. New Drugs 37 (2019) 973–983.
[37] P. Collery, A. Mohsen, A. Kermagoret, S. Corre, G. Bastian, A. Tomas, M. Wei, F. Santoni, N. Guerra, D. Desmaële, J. d'Angelo, Investig. New Drugs 33 (2015) 848–860.
[38] H.-N. Zhang, W.-G. Jia, Q.-T. Xu, C.-C. Ji, Inorg. Chim. Acta 450 (2016) 315–320.
[39] S. Ghosh, S.E. Kabir, S. Pervin, G.M.G. Hossain, D.T. Haworth, S.V. Lindeman, T. A. Siddiquee, D.W. Bennett, H.W. Roesky, Z. Anorg. Allgem. Chem. 635 (2009) 76–87.
[40] S. Ghosh, S.E. Kabir, S. Pervin, A.K. Raha, G.M. Golzar Hossain, D.T. Haworth, S. V. Lindeman, D.W. Bennett, T.A. Siddiquee, L. Salassa, H.W. Roesky, Dalton Trans. (2009) 3510–3518.
[41] J.M. Smieja, C.P. Kubiak, Inorg. Chem. 49 (2010) 9283–9289.
[42] V.K. Landry, M. Minoura, K. Pang, D. Buccella, B.V. Kelly, G. Parkin, J. Am. Chem. Soc. 128 (2006) 12490–12497.
[43] O.V. Dolomanov, L.J. Bourhis, R.J. Gildea, J.A. Howard, H. Puschmann, J. Appl. Crystallogr. 42 (2009) 339–341. https://scripts.iucr.org/cgi-bin/paper?kk5042.
[44] G.M. Sheldrick, Acta Crystallogr. A 71 (2015) 3–8. https://scripts.iucr.org/cgi-bin/paper?sc5086.
[45] G.M. Sheldrick, Acta Crystallogr. C: Struc. Chem. 71 (2015) 3–8. https://scripts.iucr.org/cgi-bin/paper?fa3356.
[46] G.R. Fulmer, A.J. Miller, N.H. Sherden, H.E. Gottlieb, A. Nudelman, B.M. Stoltz, J. E. Bercaw, K.I. Goldberg, Organometallics 29 (2010) 2176–2179.
[47] https://www.chemicalbook.com/SpectrumEN_60-56-0_1HNMR.htm.
[48] G. Vampa, S. Benvenuti, F. Severi, L. Malmusi, L. Antolini, J. Heterocyclic Chem. 32 (1995) 227–234.
[49] B. Salignac, P.V. Grundler, S. Cayemittes, U. Frey, R. Scopelliti, A.E. Merbach, R. Hedinger, K. Hegetschweiler, R. Alberto, U. Prinz, Inorg. Chem. 42 (2003) 3516–3526. https://pubs.acs.org/doi/10.1021/ic0341744.
[50] M. Minoura, V.K. Landry, J.G. Melnick, K. Pang, L. Marchiò, G. Parkin, Chem. Commun. (2006) 3990–3992.
[51] R. Garcia, A. Paulo, Â. Domingos, I. Santos, J. Organomet. Chem. 632 (2001) 41–48. https://www.sciencedirect.com/science/article/abs/pii/S0022328X01008385.
[52] A. Vlček, in: A.J. Lees (Ed.), Topics in Organometallic Chemistry: Photophysics of Organometallics, Springer - Verlag, Berlin, Heidelberg, 2010, pp. 73–114. https://link.springer.com/chapter/10.1007/3418_2009_4.
[53] K. Srinivas, C. Naga Babu, G. Prabusankar, Dalton Trans. 44 (2015) 15636–15644.
[54] H.V. Huynh, Chem. Rev. 118 (2018) 9457–9492.
[55] S.V.C. Vummaleti, D.J. Nelson, A. Poater, A. Gómez-Suárez, D.B. Cordes, A.M. Z. Slawin, S.P. Nolan, L. Cavallo, Chem. Sci. 6 (2015) 1895–1904. https://pubs.rsc.org/en/content/articlelanding/2015/sc/c4sc03264k.
[56] A. Liske, K. Verlinden, H. Buhl, K. Schaper, C. Ganter, Organometallics 32 (2013) 5269–5272.
[57] F.L. Thorp-Greenwood, R.G. Balasingham, M.P. Coogan, J. Organomet. Chem. 714 (2012) 12–21.
[58] V. Fernández-Moreira, F.L. Thorp-Greenwood, A.J. Amoroso, J. Cable, J.B. Court, V. Gray, A.J. Hayes, R.L. Jenkins, B.M. Kariuki, D. Lloyd, C.O. Millet, C.F. Williams, M.P. Coogan, Org. Biomol. Chem. 8 (2010) 3888–3901.
[59] C. Otero, A. Carreño, R. Polanco, F.M. Llancalahuen, R. Arratia-Pérez, M. Gacitúa, J.A. Fuentes, Front. Chem. 7 (2019), 1-12, 454, https://www.frontiersin.org/articles/10.3389/fchem.2019.00454/full.
[60] N. Wiratpruk, G.K. Bindra, A. Hamilton, M.D. Hulett, P.J. Barnard, Dalton Trans. 51 (2022) 7630–7643.